

## MICROMECHANICAL CONSIDERATIONS OF PARTICLE BREAKAGE USING DISCRETE ELEMENT METHOD

A. A. Mirghasemi, Department of Civil Engineering, Faculty of Engineering, University of Tehran, Tehran, Iran  
E. Seyed Hosseininia, Department of Civil Engineering, Faculty of Engineering, University of Tehran, Tehran, Iran

### ABSTRACT

Using DEM (Discrete Element Method), a model is presented to simulate the breakage of two-dimensional polygon-shaped particles. In this model, shapes of the particles generated after breakage are predefined and each uniform (uncracked) particle is replaced with smaller inter-connected sub-particles. If the bond between these sub-particles breaks, breakage will happen. With the help of this model, it is possible to study the influence of particle breakage on macro and micro mechanical parameters. In this simulation, the evolution of microstructure in granular assemblies can be seen by tracing of coordination number during the shear process. Also variation of contact normal, normal force and tangential force anisotropy can be tracked. For this purpose, two series of biaxial test simulations (breakage is enabled and disabled) are conducted on assemblies of two-dimensional polygon-shaped particles and the results are compared. It is found that the simulation results are in good agreement with observations obtained from experimental tests.

### 1. INTRODUCTION

Stability of soil structures such as breakwaters and rockfill dams is in concern of shear parameters and the behavior of granular media. In general, shear resistance and behavior of granular materials depends on different factors such as mineralogical composition, particle grading, size and shape of particles, fragmentations of particles and stress conditions.

In such high earth structures, the underlying layers bear significant weight of the upper layers, the soil grains in the underlying layers are subjected to significant stress magnitudes. The induced high stresses may cause the particles to be broken. Particle breakage and crushing of large particles to smaller ones, results in changes in grain size (gradation) curve; therefore, the mechanical behavior of granular material alters.

In this paper the results of performed tests for simulating particle breakage using Discrete Element Method is presented and the assembly behavior in terms of macroscopic and microscopic parameters is discussed.

### 2. REVIEW

Influence of particle breakage on internal friction angle and deformability of granular materials can be studied using experimental tests such as Triaxial and unconfined compression tests (Marsal 1967, Bertacchi et al. 1970, Fumagali et al. 1970, and Marachi et al. 1972, Ansari & Chandra 1986, Venkatachalam 1993, Varadarajan et al. 2003). Marshal (1967) by performing Triaxial compression tests on coarse granular materials found out that the most important factor affecting both shear strength and compressibility is the phenomenon of fragmentation undergone by a granular body when subjected to change in its state of stress both during uniform compression stage

and during deviatoric load application. Also the results showed that in granular media, the compressibility is a consequence of complex phenomenon that takes place as a result of displacements between particles combined with the particle breakage. Varadarajan et al. (2003) have investigated the behavior of two dam site rock materials (Ranjit Sagar and Purulia) in Triaxial compression tests which the former consisted of rounded and the latter angular particles. It is interesting to note that the volume change behavior of two rockfill materials was significantly different from each other. During the shearing stage of the triaxial test, compression, rearrangement and breakage of particles took place. The rounded material exhibited continuous volume compression, while the angular particles dilated and expanded after initial compression in volume. Granular materials provide a high degree of interlocking and cause dilation during shearing. Also they observed that a greater degree of particle breakage occurs with the larger particles because of the greater force per contact (Lame and Whitman 1969). There are two factors governing on the shear resistance as interlocking between particle and particle breakage. The effect of increase in interlocking is to increase the shearing resistance, while the effect of breakage of particles is vice versa. Also it is noted that angular particles are more susceptible to break than rounded particles.

Performing such tests on material with large particles in order to study the behavior of materials such as rockfill would be costly due to the required large size of specimen. At the present research, an investigation is made to study the influence of particle breakage on behavior of granular media.

In recent years, along with the progress of numerical methods and computer technology, different methods have been used to model breakage of brittle bodies with the help of Discrete Element Method (DEM). Among these methods, are the approach used by Cundall (1978), the method based

on simultaneous utilization of Molecular Dynamics (MD) (Kun et al. 1996) and the 3D approach used by Robertson & Bolton (2001) and McDowell & Haireche (2002).

### 3. PARTICLE BREAKAGE SIMULATION IN DEM

Prior to description of the methods used at the present research, a brief overview of the above methods is presented.

#### 3.1. Background

Cundall who is a pioneer in use of DEM in studying behavior of granular media and stability of rock slopes prepared a code called RBMC in which breakage mechanism of rock blocks was simulated similar to that of Brazilian test (Cundall et al. 1978, Cundall et al. 1985). In this code, in each cycle of simulation all of the point loads applied to each block are checked and then the application point and magnitude of the two maximum loads, which are applied in opposite direction of each other, are determined.

RBMC is based on the conception that particle breakage happens instantly (during one cycle) and the block is divided into two pieces through the line connecting application point of the loads. In this method, after each breakage occurrence, the primitive block is omitted and two blocks with new geometry are generated; thus it is necessary to calculate the geometry, mass and moment of inertia of these new particles and save them in the computer memory. The most recent studies in the area of breakage modeling and crack formation in brittle bodies are based on simultaneous use of DEM and MD (Kun et al. 1996). Molecular Dynamics is a computational technique that considers a macroscopic material as an assemblage of microscopic particles.

In order to study the process of fragmentation in two dimensional brittle blocks and observing the relationship of the size of broken parts with one another, Kun and Herrmann (1996) considered each block as a mesh of inter-connected tiny cells located in a plane. This cellular mesh is generated by the use of a random process (Voronoi Construction). Each cell is a rigid convex polygon that as the smallest component of the block neither breaks nor deforms and acts as a distinct element of other cells. Cells have one rotational and two linear degrees of freedom in the block plane and their behavior in contact is simulated by DEM.

In order to keep the unity of the cells forming a block, the center of mass (center of area) of each cell is connected to the mass center of neighboring cells through an elastic beam. If at a specific time during the simulation, the relative displacement between two cells enlarges so much that the stress formed in the beam connecting them exceeds the beam bearing capacity, the bond will be broken. This is the starting point in crack formation and the crack enlarges gradually as the beams connecting the consequent particles break. When an assemblage of inter-connected cells is thoroughly disconnected from the primitive block, breakage

has occurred. In the recent model, it is feasible to study the process of crack formation in a brittle body.

In order to simulate three-dimensional crushable soils, an approach is produced using DEM. In this method, agglomerates are made by bonding elementary spheres in 'crystallographic' arrays and by giving each sphere an existence probability of 0.8. This approach is used in the program PFC<sup>3D</sup> (Itasca Consulting Group, 1999). This program uses the soft contact approach of the distinct element methods, which assumes that each element has a finite normal stiffness and represents elastic flattening at contacts by allowing the bodies to overlap. A stiffness model, a bonding model and slip model are included in the constitutive representation of contact points between the elementary spheres that are the basic building block. In the linear contact model, it is assumed that each sphere have a normal and a shear stiffness. The simple contact bond can be envisaged as a pair of elastic springs at a point of glue. It serves to limit the total normal and shear forces that the contact can carry by enforcing bond-strength limits. The maximum tensile force that the bond can sustain in tension and the maximum shear force it can withstand before breaking are specified when the bond is created and may be modified at any time during the simulation. The bond breaks if either of these values is exceeded. As the simple contact bond acts over a vanishing small area of contact point, it does not resist bending moment. This means that it has no resistance to rolling of a sphere bonded adjacent to it if no third body exists to restraint the motion. This approach has been used by Robertson & Bolton (2001) and McDowell & Haireche, (2002).

A slip model acts between unbonded objects in contact, or between bonded objects when their contract breaks. It limits the shear force between objects in contact and allows slip to occur at a limiting shear force, governed by Coulomb's equation.

This approach has been accomplished for simulation of silica sand grains and the results compared with the real data for silica sand. (Cheng, Nakata & Bolton, 2003)

#### 3.2. Breakage Modeling in This Research

In the present research, simulation of biaxial test is performed on assemblies of 500 particles within 1500 sub particles using personal computer (PC). For this purpose, the program POLY (Mirghasemi et al. 1997) which is a modified version of DISC (Bathurst, 1985), to simulate two-dimensional polygon-shaped particles, is developed to model assemblies of irregularly shaped particles with the ability of breakage. (Mousavi Nik, 2000 and Seyedi Hosseininia, 2004).

It has been tried to model the particle breakage in a way that less number of particles and computational effort are needed (Mousavi Nik, 2000). In this method it is assumed that each rockfill particle can break through pre-defined straight lines with certain direction and position. The lines are determined in a way that two commonly observed behavior can be simulated. These two kinds of behavior are cracking of particle vertexes and cracking across a particle

that divides particle into pieces. For example, according to Figure 1.a, it is assumed that the particle P can only break through the lines  $d_1$ ,  $d_2$  and  $d_3$ ; therefore shape of the particles obtained from breakage of the primitive particle is specified from the beginning. Thus in this method, each uncracked particle like P consists of smaller bonded particles like  $P_1, P_2, \dots$  and  $P_n$ . Particle P is called the Base Particle and the particles  $P_1$  to  $P_n$  are called Sub-Particles. The sub-particles are considered to be rigid bodies. They are not breakable and not deformable. The base particles are not deformable but they are breakable. The both base and sub-particles are arbitrarily convex polygon shaped.

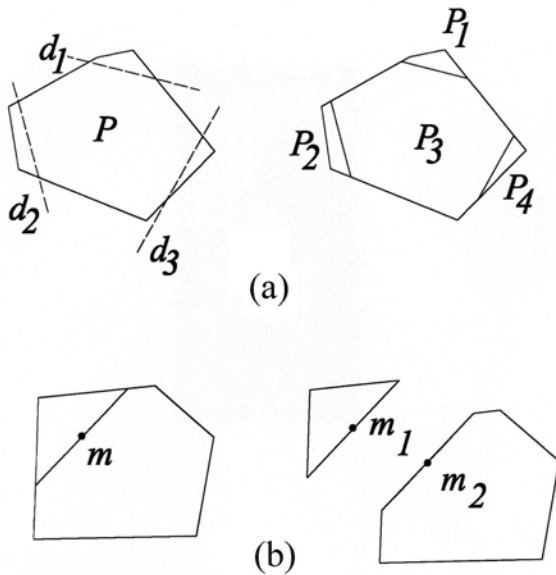


**Fig.1. Breakage modeling**  
(a). Base particle P and its sub-particles.  
(b). The bond points of two adjacent sub-particles.

Each base particle consists of several sub-particles. In order to ensure the rigidity and continuity of the base bonded particles, it is assumed that each of the two adjacent sub-particles is connected with a fixed connection at the middle of their common edge (Points  $m_1$  and  $m_2$  in Figure 2.b). This fixed connection plays the role of the bond between two bonded sub-particles. If at a specific time during the simulation, the stress formed in the connection exceeds its final bearing capacity, the connection will break and with separation of the two bonded particles from each other, breakage takes place.

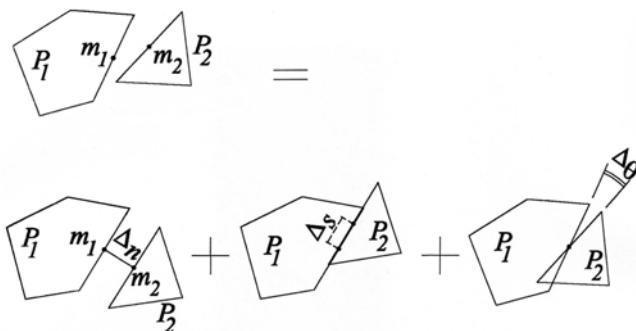


**Fig.2. Replacement of the relative displacement of two sub-particles with three normal, shear and rotational components**

For modeling the fixed connection between two bonded particles, two transitional and one rotational spring are introduced. One of the transitional springs that are perpendicular to the common face of particles is called the normal spring and the other one which is parallel to the common face is the shear spring. Moment and forces at the connection between two bonded particles are transferred through rotational and transitional spring, respectively. They can be calculated according to relative displacement of two sub-particles at each simulation cycle.

Figure 2 illustrates a base particle P in an assembly of particles subjected to an arbitrary loading. Due to interaction between particles, the forces and moments are induced at base particle's contact points. As a consequence, it is observed that the sub-particles  $P_1$  and  $P_2$  are relatively displaced against each other because of the induced contact forces with adjacent particles. Consequently, the points  $m_1$  and  $m_2$  are no longer coincident with each other. To determine the force and moment applied on each sub-particle, the relative displacement of the two sub-particles  $P_1$  and  $P_2$  is replaced with its three components,  $\Delta_n$  (normal displacement),  $\Delta_s$  (shear displacement) and  $\Delta_\theta$  (rotational displacement) (Figure 2). Hence, the normal and shear forces and the moment at the contact point can be expressed as follows:

$$\begin{aligned} F_{n-Bond} &= K_{n-Bond} \cdot \Delta_n \\ F_{s-Bond} &= K_{s-Bond} \cdot \Delta_s \\ M_{Bond} &= K_{\theta-Bond} \cdot \Delta_\theta \end{aligned} \quad [1]$$

where  $K_{\theta-Bond}$  is the stiffness of the rotational spring and  $K_{n-Bond}$  and  $K_{s-Bond}$  are unit length stiffness of the normal and shear springs, respectively. Values of these parameters are considered to be proportional to the stiffness of the particles. With the existence of one of the two following conditions, the bond between the two adjacent sub-particles is omitted and the breakage will happen:

1. If the stress at the bond between the two particles is larger than the allowable shear stress (the bond bearing capacity).
2. If the maximum compressive and tensile stresses caused by moment and normal force of the bond exceeds the allowable compressive and tensile stress of the bond.

The bond bearing capacity obeys from the Coulomb failure criterion for rocks which is extended in both compressive and tensile stresses but they are limited by magnitudes of stresses obtained from unconfined compressive strength and Brazilian tensile strength tests respectively (Seyedi Hosseininia, 2004).

The same slip model acts between unbonded sub particles in contact, or between bonded objects when their contact breaks but no limit in the upper bound for compressive

strength exists. The greater the normal stress on the slip surface, the stronger is the shear resistance. If the shear force between objects in contact exceeds the resistance, slip occurs.

#### 4. TEST SIMULATIONS

In order to investigate the particle breakage in a granular media two tests were performed. In the test A particles are rigid with no ability in fragmentation while in the test B the rigid particles are substituted by bonded sub-particles in order to be breakable.

Each test includes three stages. At first, the initial computer-generated assembly of particles (Fig.3 (a)) was compacted, then subjected to a pre-defined confining pressure of 2.0 MPa and finally the assembly was sheared biaxially at a constant deviatoric strain rate. The inter-particle friction coefficient is set to 0.5 for all tests and the particles are assumed to be cohesionless at the contact.

The parameters used for tests A and B are summarized in Table 1 and 2, respectively.

**Table 1. Parameters used in test A  
(Breakage disabled)**

Normal and tangential stiffness (N/m)	$2.0 \times 10^7$
Unit weight of particles ( $\text{kg/m}^3$ )	2500
Translational damping coefficient (1/sec)	75
Rotational damping coefficient (1/sec)	450
Time step (sec)	$3.2 \times 10^{-4}$
Strain rate	0.005

**Table 2. Parameters used test B  
(Breakage enabled)**

Normal and tangential stiffness (N/m)	$2.0 \times 10^7$	
Unit weight of particles ( $\text{kN/m}^3$ )	2500	
Translational damping coefficient (1/sec)	150	
Rotational damping coefficient (1/sec)	900	
Time step (sec)	$1.52 \times 10^{-4}$	
Strain rate	0.005	
Module of elasticity (E) ( $\text{MN/m}^2$ )	$9.0 \times 10^4$	
Rock Strength Parameters	Compressive Strength ( $\text{MN/m}^2$ )	350
	Tensile Strength ( $\text{MN/m}^2$ )	35
	Intercept ( $\text{MN/m}^2$ )	75
	Coefficient of Static Friction	1.60

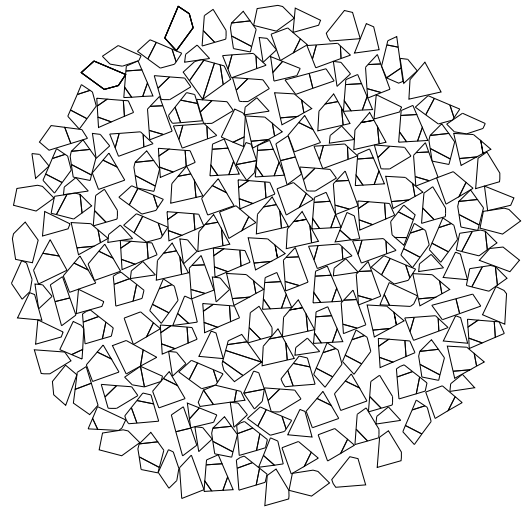
#### 5. TEST RESULTS

The results obtained from the simulations can be studied from two different points of view as macro and micromechanical considerations.

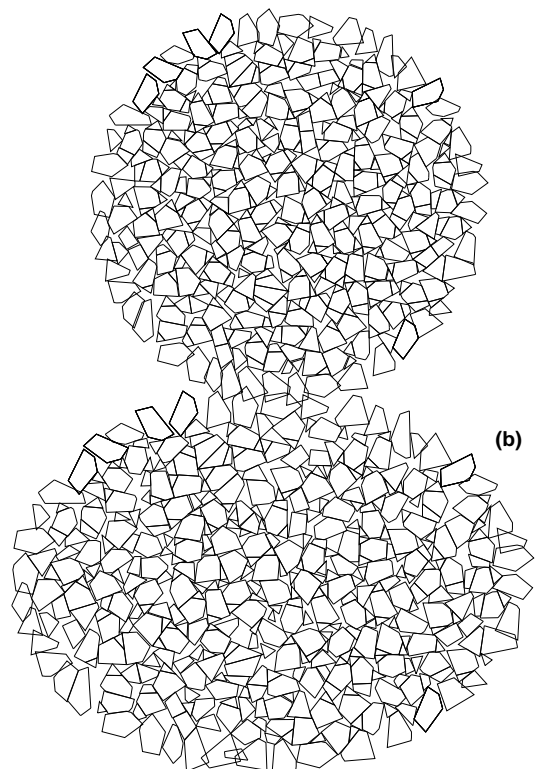
##### Macromechanical Observations

The results of biaxial simulations in tests A and B are presented in the form of curves of  $\sin \phi$  mobilized (Equation 2) versus axial strain (Fig.4.a) and volumetric strain versus axial strain (Fig.4.b).

As shown in both tests, the shear strength ( $\sin \phi$  mobilized), which is in term of the principal stress ratio, increases and then reaches to a constant value.



(a)



(b)

(a)

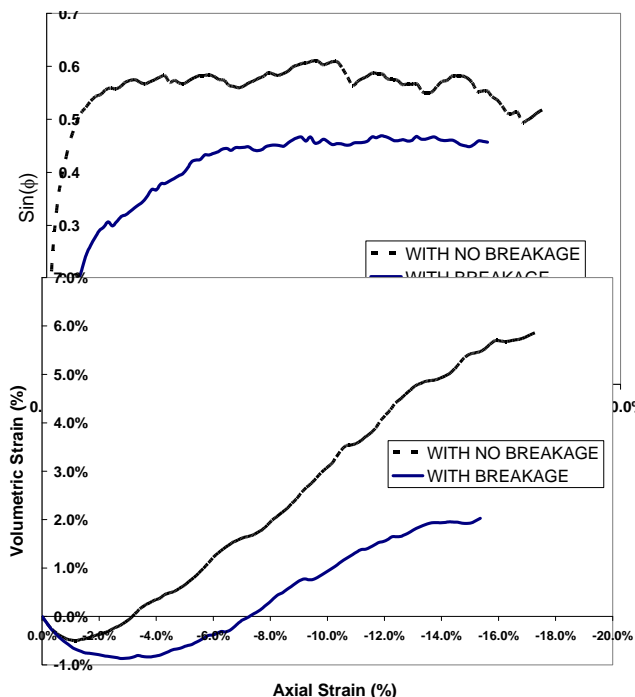
(c)

**Fig.3. Three simulation stages for breakable particles**  
(a) Initial generated assembly of particles,  
(b) Isotropically compacted assembly,  
(c) Sheared assembly at last stage of biaxial test (after Seyedi Hosseininia, 2004).

In test A, the  $\sin \phi_{\text{mobilized}}$  grows rapidly and reaches at a peak of 0.6, but in test B, it gradually increases and it becomes constant just under 0.5. It seems that particle breakage has a decreasing effect on shearing resistance of the assembly.

$$\sin \phi = \frac{\sigma_1 - \sigma_3}{\sigma_1 + \sigma_3} = \frac{\sigma_1 / \sigma_3 - 1}{\sigma_1 / \sigma_3 + 1} \quad [2]$$

In general, the angular particles have dilative behavior (sharma, 1967; Varadarajan et al., 2003). Figure 4.b shows that the assembly with no breakage has a more dilative behavior than that with the ability of fragmentation. As investigated before, the more the assembly dilates, the larger is the shear resistance. In test B, particles cannot undergo the forces imposed on them and breakage happens, therefore smaller particles fill the voids and let the other particles move freely. This causes the assembly to show a compressive behavior in larger axial strains followed by increasing volumetric strain. This trend can justify the reduction of  $\sin \phi_{\text{mobilized}}$  in test B. The same result has been obtained in experimental test results (Marshall, 1967, Furnagalli et al., 1970).



(b)

**Fig.4. Relationship between  $\sin \phi_{\text{mobilized}}$  and axial strain**

Figure 5 illustrates the variation of particle breakage in three modes of failure which have been tracked during biaxial shear test. The possible causes of fragmentations are due to compression, tension and shear breakage. It shows that no particle breakage has happened due to compression. Although in confining pressure stage, most particles have been broken because of shear failure (35%), in biaxial test the degree of tension breakage is higher which started from about 13% at the beginning and it reached at just below 40%. Also the number of shear breakage is to some extent constant at large axial strain whereas the tension breakage grows gradually.

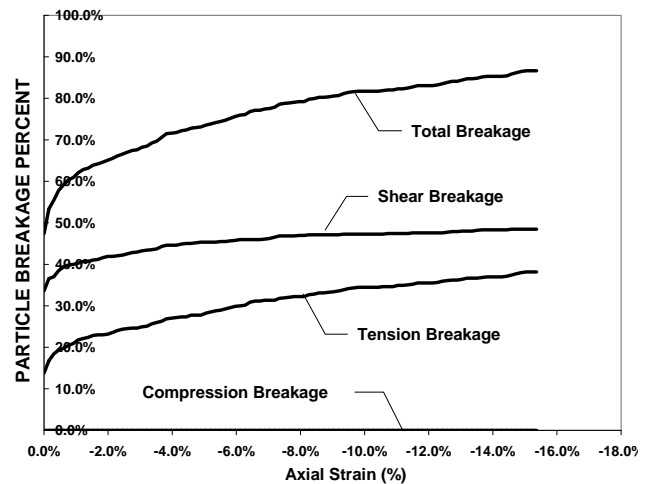


**Fig.5. Relationship between particle breakage and axial strain**

Having performed Triaxial tests on rockfill, Marsal (1973) showed that at the beginning of the test, larger particles that contain more flaws and defects, break and it is why the breakage rate at the beginning of the test is high. At the primitive stages of the test, the smaller particles, produced by larger particles breakage, are located in the voids

between the other intact large particles and consequently have no role in transferring the force to their neighboring particles. After compaction of assembly during next stages, the gaps between particles become smaller and the small particles can play their role in transferring the force to the adjacent particles. Thus the mean contact stresses decrease owing to the increase of particles surrounding each grain; therefore, the breakage quantity will reduce afterwards. Considering the total number of breakage in Figure 5, the rate of particle breakage is high at the beginning of simulation and then it slows down. Therefore variation of breakage rate versus axial strain (and consequently axial stress) during the simulated biaxial test is in agreement with the trend observed by Marsal (1973). Also, variations of  $\sin \phi_{\text{mobilized}}$  and volumetric strains with different confining pressures, considering particle breakage have been studied (Mirghasemi et al, 1997, Mousavi Nik, 2000). It is found that  $\sin \phi_{\text{mobilized}}$  falls with increasing confining pressure while the dilatancy acts vice versa.

## 5.2. Microscopic Behavior

While it is obvious that forces in granular media must be carried by means of contacts between particles, it is only recently that a means of quantifying the arrangement of contacts has been developed. For any angle  $\theta$ , the portion of the total number of contacts in the system that are oriented at angle  $\theta$  is  $E(\theta)$ . The distribution of contact normal orientations is described by a function such that the fraction of all assembly contact normals falls within the orientation interval  $\Delta\theta$ . Rothenburg (1980) showed that the distribution of such contacts takes the form

$$E(\theta) = \frac{1}{2\pi} [1 + a \cos 2(\theta - \theta_0)] \quad [3]$$

where  $a$  is referred to as the parameter of anisotropy, and  $\theta_0$  is the major principal direction of anisotropy. The meaning of  $a$  becomes clear if it is noted that the number of contacts oriented along the direction of anisotropy, i.e. when  $\theta = \theta_0$  is proportional to  $1 + a$  while the number of contacts oriented in the perpendicular direction is proportional to  $1 - a$ . The parameter  $a$ , therefore, is proportional to the difference in the number of contacts oriented along the direction of anisotropy and in perpendicular direction.

A similar expression was introduced by Thornton & Barnes (1986). The magnitudes of the contact forces in an assembly with irregular geometry vary from contact to contact. Despite the apparent randomness in the variation of contact forces, regular trends emerge when they are averaged over groups of contacts with similar orientations. The average contact force acting at contacts with an orientation can be decomposed into an average normal force component,  $\bar{f}_n^c(\theta)$ , and an average tangential force component,  $\bar{f}_t^c(\theta)$ . By averaging the contact forces of the contacts falling within the group of similar orientation and following the same logic as for the contact normals, symmetrical second-order tensors may be introduced to

describe average normal contact forces and average tangential contact forces. The average normal contact force tensor can be defined as (Bathurst, 1985)

$$\bar{f}_n(\theta) = \bar{f}_n^0 [1 + a_n \cos 2(\theta - \theta_f)] \quad [4]$$

where  $a_n$  is the coefficient of normal force anisotropy, and  $\theta_f$  is the major principal direction of force anisotropy;  $\bar{f}_n^0(\theta)$  is the average normal contact force from all assembly contacts.

The average tangential contact force tensor can be defined as:

$$\bar{f}_t(\theta) = -f_t^0 [a_t \sin 2(\theta - \theta_0)] \quad [5]$$

where  $a_t$  is the coefficient of tangential force anisotropy and  $\theta_0$  the direction of anisotropy.

The general expression for the average stress tensor can now be written as

$$\sigma_{ij} = m_v l_0 \int_0^{2\pi} [\bar{f}_n^c(\theta) n_i^c n_j^c + \bar{f}_t^c(\theta) t_i^c n_j^c] E(\theta) d\theta \quad [6]$$

where  $m_v$  is the average number of contacts per unit area (volume),  $l_0$  is the assembly average contact vector length (average distance from the particle centroid to the contact point),  $n_i^c$  is the contact normal vector, and  $t_i^c$  is the contact tangent vector. Rothenburg & Bathurst (1989, 1992) derived a relationship between the measure of shear stress and the parameters  $a$ ,  $a_n$ ,  $a_t$  involved in the characterization of anisotropies in contact orientations and contact forces according to equations (2)-(5). For the case when the directions of anisotropy in contact forces and contact orientations coincide, as in a biaxial test, the relationship is as follows:

$$\left( \frac{\sigma_1 - \sigma_2}{\sigma_1 + \sigma_2} \right) = \left( \frac{a + a_n + a_t}{2 + a_n + a_t} \right)$$

the parameters  $a$ ,  $a_n$ ,  $a_t$  involved in the characterization of anisotropies in contact orientations and contact forces according to equations (2)-(5). For the case when the directions of anisotropy in contact forces and contact orientations coincide, as in a biaxial test, the relationship is as follows:

$$[7]$$

The simplified expression suggests that the capacity of a cohesionless granular assembly to carry deviatoric loads is directly attributable to its ability to develop anisotropy in contact orientations or to withstand directional variations of average contact forces. All contributions to deviatoric load capacity are assumed to be additive. Thornton & Barnes (1986) also introduced a partitioning of the stress tensor into various contributions using somewhat different micromechanical averages. From a physical point of view, the most significant result of this investigation is the introduction of parameters that quantify essential features of microstructure such as anisotropy in contact orientations and average contact forces. Equation (7) appears to be a remarkably simple relationship that is directly verifiable and conveys a clear statement of the additive contributions of different mechanisms of load transmission to the shear capacity of granular materials. Although equation (7) was derived originally for disc-shaped particles and was subsequently extended for assemblies of elliptical particles,

it is shown, based on numerical simulations, that the equation is sufficiently accurate for assemblies of angular particles as well (Mirghasemi et al., 1997). This equation is evaluated too for the media in which the particles have the ability of breakage.

A general idea of how the microstructure in the granular assemblies evolves during the shearing process may best be conveyed from the change in the number of contacts in the assembly or the average coordination number of the system.

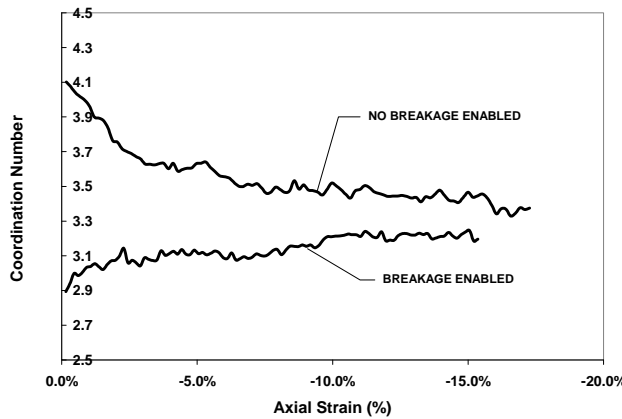


Fig. 6. Relationship between average coordination number and axial strain

Fig. 6 presents the evolution of the average coordination number during shear deformation.

At the beginning of each test, some contacts were created owing to the elastic compression from the increase in the hydrostatic stress. As shown in figure 6, the coordination number for the assembly with the ability of breakage is about three quarters of the same assembly in which particles cannot break. Also the trends are different from each other during shearing process. In test A, the number of contacts per total number of particles decreases rapidly with axial strain and reaches at about 3.5, while the coordination number in test B, grows very gradually from 2.9 to 3.3 during the biaxial test that it is like to be constant.

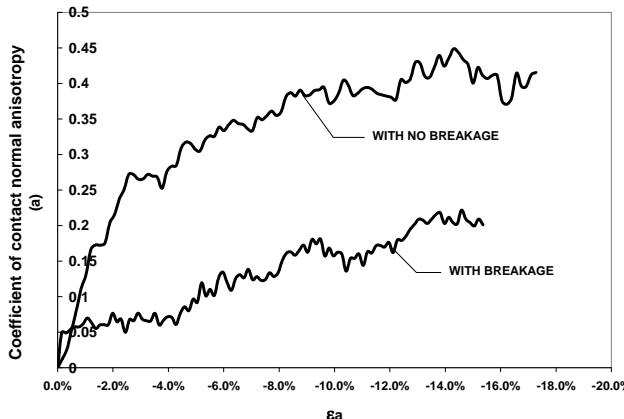
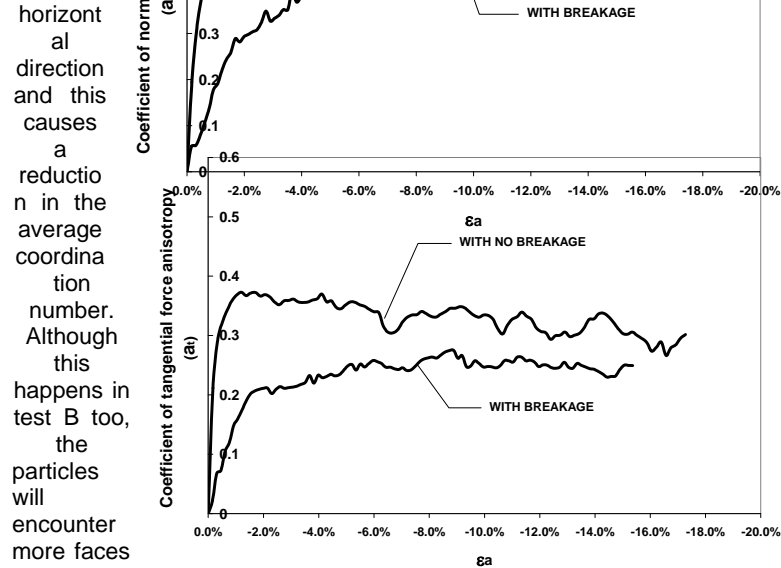


Fig. 7. Evolution of contact normal anisotropy coefficient

In test A, in which the particles can not break, the contacts began to degrade as the axial stress increased, mainly in the horizontal direction and this causes a reduction in the average coordination number. Although this happens in test B too, the particles will encounter more faces to have contact with their neighboring particles due to the fragmentation. That's why the number of contacts grows.



The evolution of the contact normal anisotropy (parameter  $a$  in equation (3)) as a function of axial strain is illustrated in Fig. 7. This coefficient is essentially proportional to the difference in the number of contacts in each direction, and describes the degree of anisotropy in contact orientations.

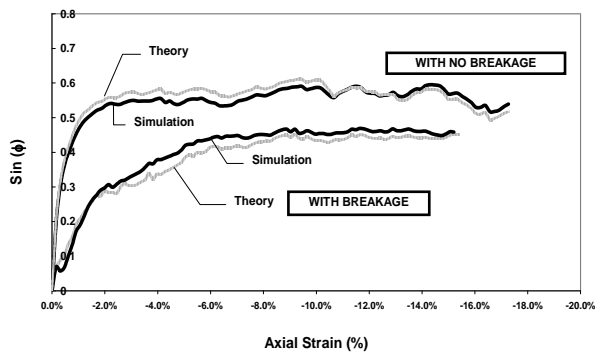
The coefficient of fabric anisotropy evolves to the maximum values as contacts, mostly oriented along the direction of tensile strain (horizontal direction), are lost. In test A, the coefficient reduces to the lower ultimate values at large axial strain, but in test B, it continuously and slowly grows to a peak value of half of that in test A.

Figure 8 presents the development of anisotropy in normal contact forces by plotting the variation of the coefficient of normal contact force,  $a_n$ , with axial strain during the simulations on assemblies with rigid and breakable particles. In both tests, by applying deviatoric axial strain in the vertical direction, the normal forces carried by chains of particles in the vertical direction are increased, while the magnitude of average normal forces in the horizontal direction remains almost constant. The parameter  $a_n$  indicates the difference in the values of average forces on vertical and horizontal contacts. A greater difference in the

magnitude of the average forces in the horizontal and vertical directions provides a higher value for  $a_n$ . In test A, as the axial strain increases,  $a_n$  shows a rapid growth at lower axial strain, followed by a reduction after the maximum value. This is because of loss of contacts and also the loss of the capacity of chains of particles to sustain high forces. In contrast to test A, when the particles can be divided into smaller ones, the parameter  $a_n$  shows a gradual increase which reaches at a constant value. This behavior of  $a_n$  is sensitive while the particles cannot tolerate the imposed forces and breakage happens, therefore, particles can not make a chain to show a peak in  $a_n$ . Although the increasing of  $a_n$  are in different manners in these two tests, it might be anticipated that  $a_n$  reaches to the same ultimate value at large axial strain.

**Fig.8. Evolution of normal force anisotropy coefficient**

The coefficient of tangential contact force anisotropy,  $a_t$ , shows a rapid rise at small axial strain. In test A, the coefficient of tangential force anisotropy reaches to the maximum value, followed by a slow reduction in magnitude, as illustrated in Fig. 9. In spite of test A,  $a_t$  in test B continues to grow very slowly to a constant value. The initial increase in  $a_t$  is due to the development of frictional resistance as a result of potential relative movement between adjacent particles. As the number of contacts reduces, the particles gain more opportunity to rotate; therefore in test A, tangential forces are slowly released. In test B, particles cannot bear the tangential forces and get into pieces so they have more opportunity to move freely in the voids between other particles. Particle breakage causes not to mobilize the shear forces completely; therefore shear force doesn't reach to a peak.



**Fig.10. Verification of relationship between stress and fabric for assembly with and without breakable particles**

The coefficients of anisotropy  $a$ ,  $a_n$  and  $a_t$  were substituted into the stress-force-fabric relationship (equation (7)) developed for assemblies of circular (Rothenburg & Bathurst, 1989) and elliptical (Rothenburg & Bathurst, 1992) particles. Also this equation sufficiently works for polygon-shaped particles (Mirghasemi et al., 1997). Figure 10 compares the computed shear resistance based on theory

(right-hand side of equation (7)) and the value of  $\sin \phi_{\text{mobilized}}$  (left-hand side of equation (7)) provided by biaxial simulations on assemblies with angular particles for both tests A and B. As can be observed, the stress-force-fabric expression is in agreement with the measured shear resistance in the test simulations.

All these tests were performed under the confining pressure of 2.0MPa. It is also interesting to note that the same trends and variations shown in both tests in which particle breakage is enabled and disabled, are obtained with different confining pressures (Seyedi Hosseininia, 2004).

## 6. CONCLUSIONS

The comparison of the two simulated series of biaxial tests with a constant confining pressure indicated that breakage of the particles leads to decrease of internal angle of friction and increase of granular material compressibility. Also the rate of particle breakage in different modes during biaxial test was investigated. The results are similar to data obtained from experimental tests on real rockfill materials.

The influence of particle breakage was studied on the variation of micromechanical parameters. The coordination number remains almost constant during the test with particles broken. As observed, the magnitude of normal contact, normal force and tangential force anisotropy coefficients are smaller in the case of breakable particles than those in rigid particles.

The stress-force-fabric expression developed by Rothenburg and Bathurst (1989, 1992) was verified for the assemblies of angular particles in which the particles can break.

Comparisons between simulations results and observations obtained from experimental tests, shows that the method presented for modeling breakage, can help us to have a qualitative view about the effect of breakage phenomenon on behavior of granular materials.

## 7. REFERENCES

- 1) Cundall, P.A. (1978). "Ball – A Computer Program to Model Granular Media Using Distinct Element Method", *Technical Note TN-LN-13.*, Advanced Technology Group, Dames and Moore, London.
- 2) Kun, F. and Herrmann, H.J. (1996). "A Study of Fragmentation Process Using A Discrete Element Method." *Comput.Methods Appl. Mech. Engrg.* 138, pp.3-18.
- 3) Marsal, R.J. (1967). "Large Scale Testing of Rockfill Materials", *J.of the Soil Mechanics and Foundation Division*, Vol.93, No. SM2.
- 4) Seyedi Hosseininia, E., "Micromechanical Considerations of Particle Breakage using Discrete Element Method", M.Sc Thesis, Tehran University, Tehran, Iran





57<sup>th</sup> Canadian Geotechnical Conference  
5<sup>th</sup> Joint IAH-CNC/CGS Conference  
Hilton Hotel, October 24-28, 2004  
Québec city, Québec, Canada

- 5) Mirghasemi, A.A., Rothenburg, L. and Matyas, E.L.(1997) Numerical Simulations of Assemblies of Two-Dimensional Polygon-Shaped Particles and Effects of Confining Pressure on Shear Strength, *Soils and Foundations*, Japanese Geotechnical Society, Vol.37, No.3, pp.43-52.
- 6) Rothenburg, L., Bathurst, R..J. & Dusseault, M.B. (1989). "Micromechanical ideas in constitutive modeling of granular materials", *Powders and Grains*, Biarez & Gourves(eds), 1989 Balkema, Rotterdam. ISBN 906191 984 3
- 7) Mirghasemi, A.A., Rothenburg, L. and Matyas, E.L.(2002) Influence of particle shape on engineering properties of assemblies of two-dimensional polygon-shaped particles, *Geotechnique* 52, No.3, 209-217
- 8) Mirghasemi, A.A., Mousavi Nik, R. (2001), "Influence of particle breakage on mechanical behavior of assemblies of two-dimensional polygon-shaped particles", "Proc. of 54<sup>th</sup> Canadian Geotechnical Conference, Calgary, Alberta, 614-620
- 9) Varadarajan, A, Sharma, K.G., Venkatachalam, K. & Gupta, A.K., "Testing and modeling two rockfill materials", *Journal of geotechnical and geoenvironmental engineering*, ASCE, March 2003
- 10) Cheng, Y.P., Nakata, Y. & Bolton, M.D. (2003), Discrete element simulation of crushable soil, *Geotechnique* 53, No. 7, 633-641.